Fermi National Accelerator Laboratory

FERMILAB-Conf-77/61-EXP
2021.000

PHOTON-HADRON INTERACTIONS: RECENT RESULTS AT FERMILAB*

Thomas Nash
Fermi National Accelerator Laboratory, Batavia, Illinois 60510

July 1977

*Submitted to the European Conference on Particle Physics, Budapest, Hungary, July 4-9, 1977.

PHOTON-HADRON INTERACTIONS: RECENT RESULTS AT FERMILAB

Thomas Nash
Fermi National Accelerator Laboratory
Batavia, Illinois 60510

I could not possibly report about photon physics at Fermilab at this time without mentioning Ben Lee. Ben was killed June 16 in a traffic accident on Interstate 80 in Western Illinois. He was on his way to the summer meeting of the Fermilab Program Advisory Committee at Aspen. The review, Search for Charm,[1] Ben wrote with Gaillard and Rosner appeared before the J/ψ discoveries and is even now a constant reference. Ben was a guiding spirit and a good friend to many of the experimenters working in photoproduction and charm physics. He was always available to talk to us and was particularly helpful to younger colleagues. Many "valuable discussions" with Ben Lee have been a strong influence in the outlook on high energy photon physics I will present today. We miss him.

The successful pursuit of photon physics at a high energy proton accelerator has been one of the happiest - and, to some, most surprising - developments at Fermilab. There are several reasons for this success and for the priority that photon physics is now receiving at Fermilab. The most important is that photons - along with neutrinos - are ideal probes for studying the new physics. Since photons couple to quark-anti quark pairs, photon beams carry the highest fraction of charmed (or other new quark flavors) of any "hadronic beam". In some sense at high enough masses the photon is 40% charm (Fig. 1). In other hadron beams charm appears only in the quark sea and its manifestation is swamped by the background from the valence - non charmed quarks. In a photon beam the

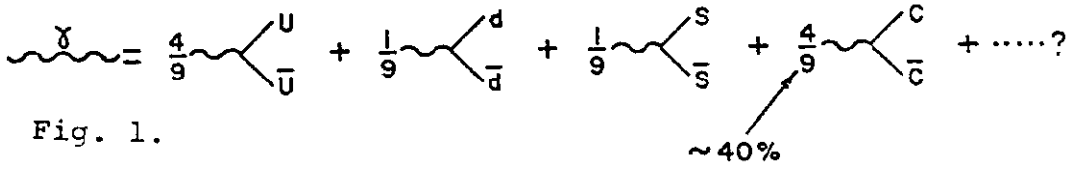

Fig. 1.

charm quark pair carries all of the momentum of the beam (x = large) unlike the charm quarks of a hadron beam which carry only a fraction of the momentum (x ≈ 0). Higher mass states are thus more readily formed by photons and at high x they are less likely to be buried in the background at low x. Also, the Lorentz transformation of angles leads to better experimental acceptance for the high x states produced by photons. Other factors aid photon physics at high energies. These include the good duty factor of high energy proton accelerators, the improvement in shower counter energy resolution which goes as $E^{-\frac{1}{2}}$, and the large acceptance experiments possible at high energy.

Lest this review sound too much like a proposal presentation, let me turn quickly to a brief description of the Fermilab photon beams. I will then report on the results the two photon experiments have produced since last summer.

There are two photon beams at Fermilab, both located in the Proton East area (Fig. 2). The beams look at two ~ 30 cm Be targets located 30 cm apart. Experiments in the two beams do not run simultaneously. Both beams start by sweeping charged particles out of the 0° neutral beam produced by p-Be interactions. The Broad Band beam then passes through 34 meters of liquid deuterium which improves the n/γ fraction in the beam by about 200. Following the deuterium the beam penetrates a 60 m long steel muon shield, the final resting place for a World War II cruiser. In order to establish that observed effects are in fact induced by photons, the experimenters in this beam are able to enhance the relative K_L and n components of the beam. By inserting 6 radiation lengths of lead after about 1/3 of the deuterium the K_L fraction is increased. To increase the neutron component the experimenters have run with only the first 1/3 of the deuterium and the Pb in place. In the Tagged Photon Beam the photons of the primary neutral beam are converted to electrons in .5 radiation lengths of lead about 12 m from the target. The e^- are then transported some 300 m to a tagging system. Collimation in the transport

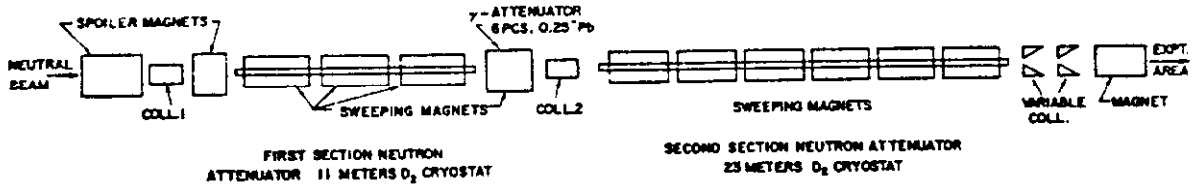

BROAD BAND BEAM

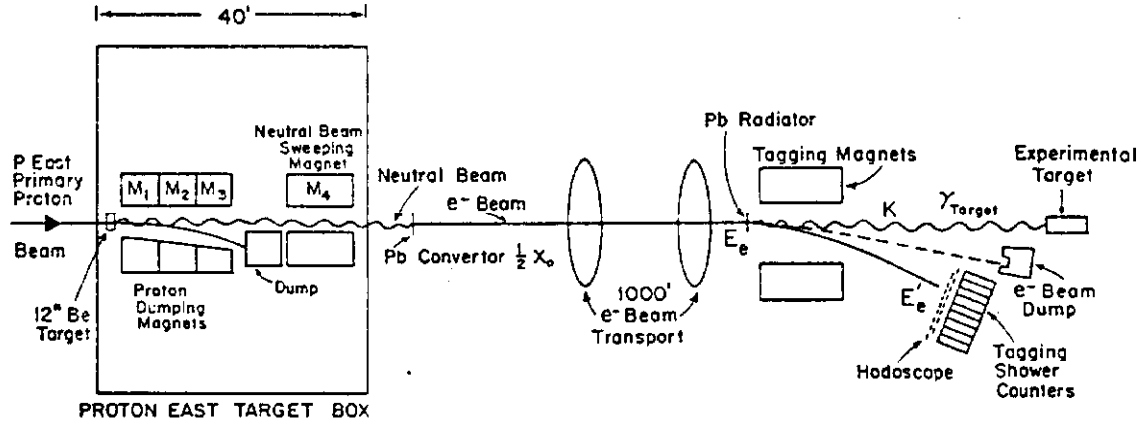

TAGGED PHOTON BEAM

Fig. 2.

helps reduce the π fraction of the beam below 0.5% and define the energy (E_e) to ± 2.5%. The electrons pass through a radiator at the tagging system and produce a bremsstrahlung spectrum of photons which head to the experimental target 25 m downstream. Three magnets bend the electrons into a bank of hodoscopes and Pb-lucite and Pb glass shower counters which measure the energy E'_e of electrons that radiate photons. The photons which radiate in the energy range $.45\ E_e < k < .9\ E_e$ can then be individually tagged with energy $k = E_e - E'_e$. The hadronic contamination (K_L,n) of the tagged photons is $< 10^{-6}$. It is reduced to this level by anti counters and the requirement that the magnetically measured momentum equal the shower energy of the radiating electrons.

Figure 3 shows the approximate photon intensity spectrum available from the beams. In the experiments that we will discuss here the Broad Band beam typically used 1×10^{12} protons/pulse and the Tagged γ beam used $3\text{-}4 \times 10^{12}$ protons/pulse. For experiments requiring the high intensities shown in Fig. 3

(J/ψ production reported last year, charm physics in the future) a thick tagging radiator (up to 20% X_o) is used. In the total cross section experiment, which I will report on shortly, requirements on precision called for much thinner radiators (typically 1% X_o) to avoid large multiple bremsstrahlung corrections.

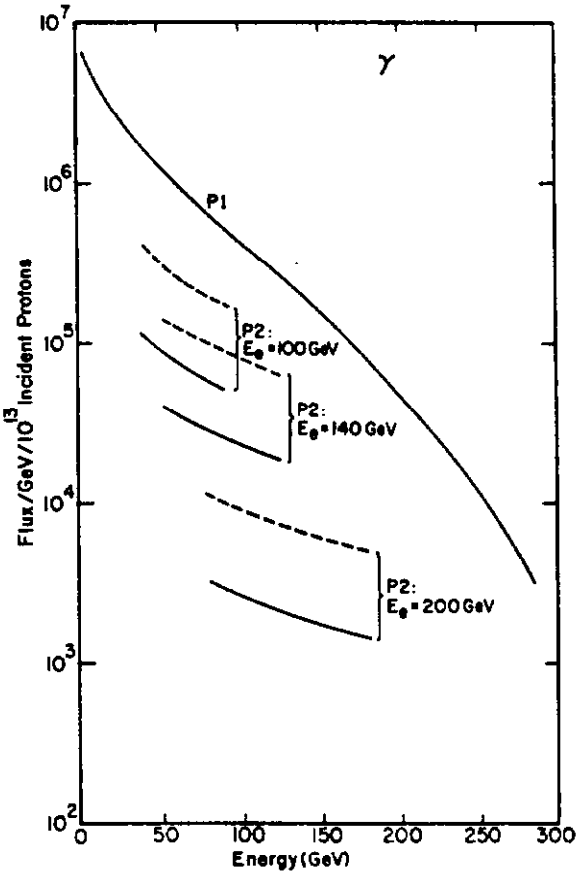

Fig. 3. P1 is Broad Band Beam. P2 is Tagged γ Beam, $.2X_o$. Dashed line is planned improvement.

Turning now to the recent experiments, let me first describe the successful search for charm in photoproduction in the Broad Band beam by a group from Columbia, Hawaii, Illinois, and Fermilab (B. Knapp, W. Lee, P. Leung (thesis), D. Smith, A. Wijangco, J. Knauer, D. Yount, J. Bronstein, R. Coleman, G. Gladding, M. Goodman, R. Messner, T. O'Halloran, J. Sarracino, A. Wattenberg, M. Binkley, I. Gaines, M. Gormley, and J. Peoples).[2] The apparatus used for this experiment which was run during Fall 1975 is shown in Fig. 4. It is substantially the same as that used a year earlier by this group in the J/ψ photoproduction experiment that established the hadronic nature of the new state.[3] Following a 2.5 cm Be target, a magnet (20 kG-m) and 5 MWPC's (each with X, U, V planes) are used for momentum analysis of charged tracks. Resolution is $\frac{\delta p}{p^2} = \pm\ 3.5 \times 10^{-4}$. There is a lead-scintillator shower detector to identify $e^{\pm}$ and γ. A hadron calorimeter identifies hadrons and measures energy to ~ 25%. It is followed by a segmented μ identifier.

Triggering was handled by the versatile Nevis pin logic system which allowed 10 simultaneous triggers (with various

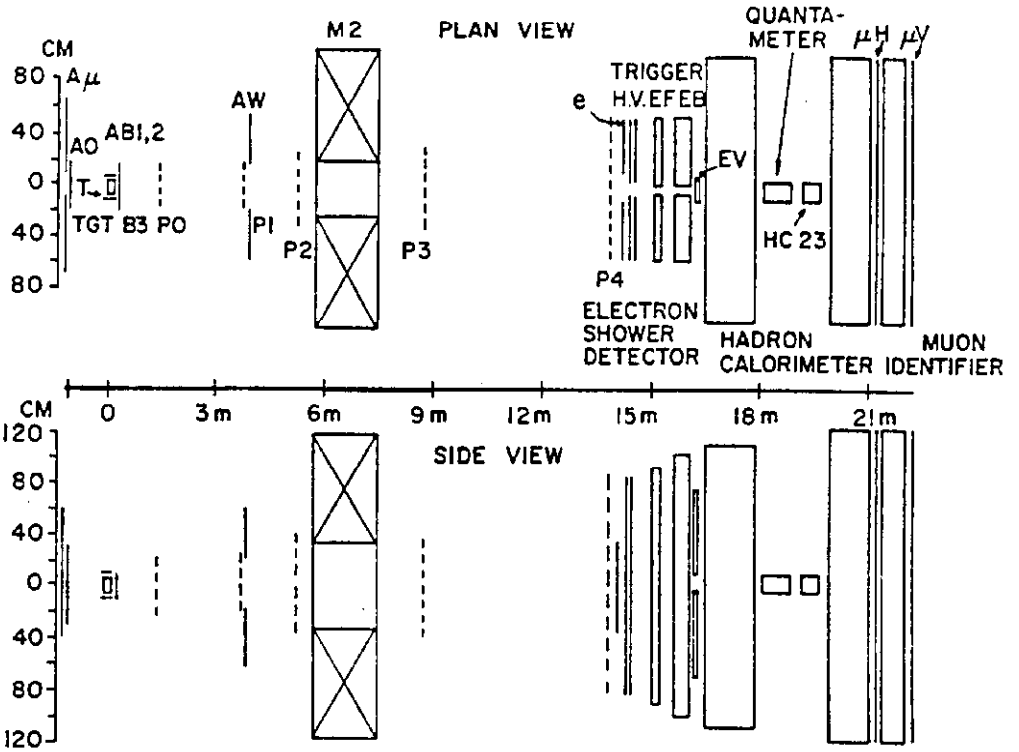

VIEWS OF MAGNETIC SPECTROMETER AND PARTICLE IDENTIFICATION SYSTEM

Fig. 4.

scaledowns). The master gate involved B3, the trigger arrays H, V, and the calorimeter. Six of the 10 triggers required leptons (1e, 1μ, 2e, 2μ, μe, 2μ + had). The other four triggers required only hadronic signatures and account for ~ 70% of the interesting physics we will describe. In all of these hadronic triggers no signal was allowed in AB or AW, anti counters which frame the magnet acceptance of about ± 35 mrad. Over 10^7 events were recorded on tape.

The analysis of the data involved first locating secondary neutral vertices in the 4 m long decay region starting 70 cm from the target. The V^O was required to intersect a charged track in the target. A beautiful K_s^O peak is seen (Fig. 5a) if the V^O track masses are taken as $m_{\pi^\pm}$. K_s^O are identified by their mass and removed from the V^O sample. The proton mass is then assigned to the more energetic track and

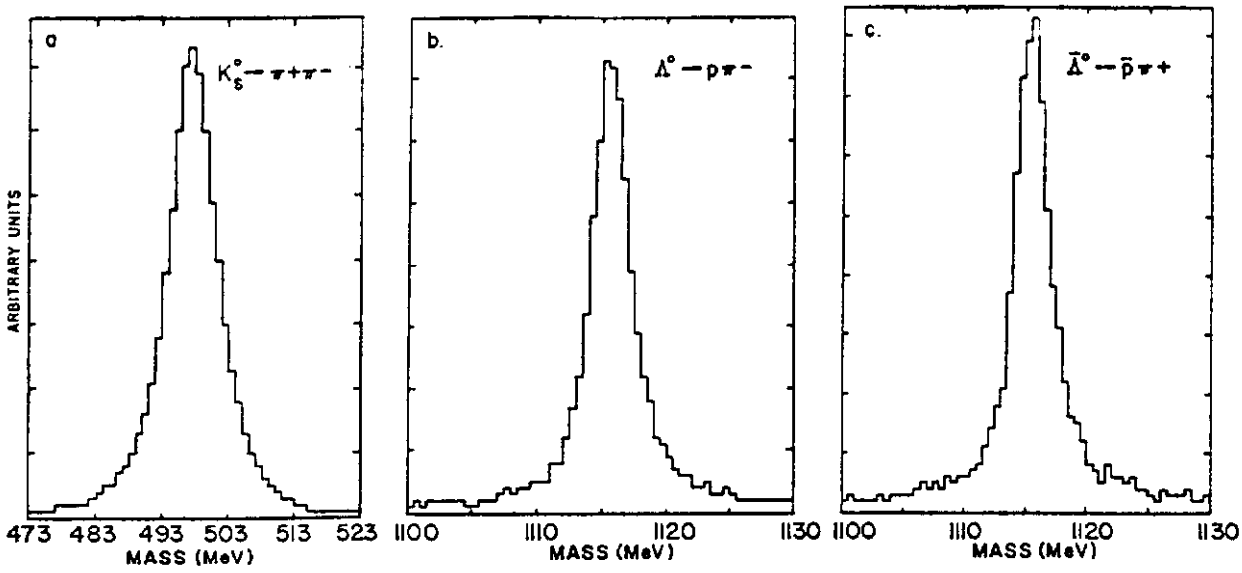

Fig. 5.

clean Λ^o and $\bar{\Lambda}^o$ peaks are found (Fig. 5b,c). The Λ^o ($\bar{\Lambda}^o$) identified from these plots have roughly 2% (4%) background, respectively. In searching for charmed states mass plots were made of $K_s + n\pi^{\pm}$, $\Lambda + n\pi^{\pm}$, and $\bar{\Lambda} + n\pi^{\pm}$ with n = 1, 2, 3, 4. These are expected to include the dominant decay modes of charmed mesons and baryons. The same data was also plotted assuming a K and a proton mass for one of the charged tracks. With the exception of the plots we show here the spectra are featureless at masses over 1.5 GeV.

There is a spectacular 7σ peak in the $\bar{\Lambda}\pi^+\pi^-\pi^-$ spectrum at 2.26 ± .02 GeV with a width of 40 ± 20 MeV (Fig. 6a). The experimental mass resolution is ~ 30 MeV so that the width is consistent with zero but not very consistent with the 100-200

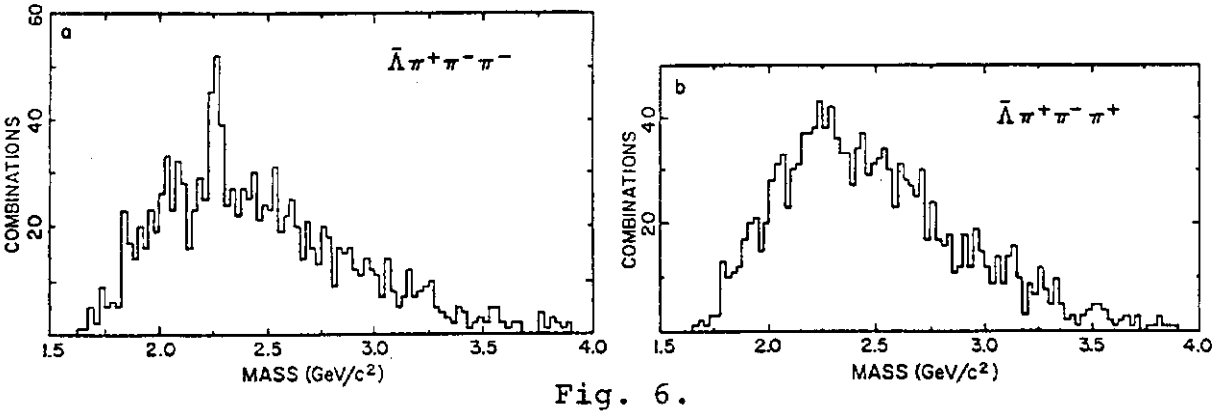

Fig. 6.

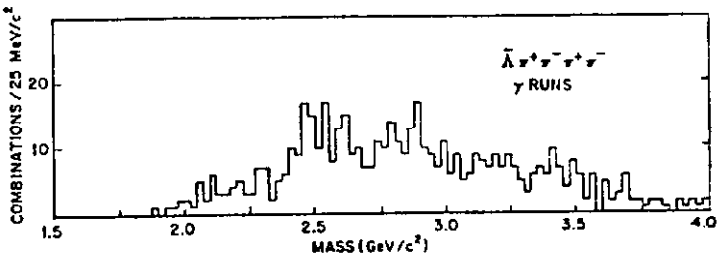

Fig. 7a.

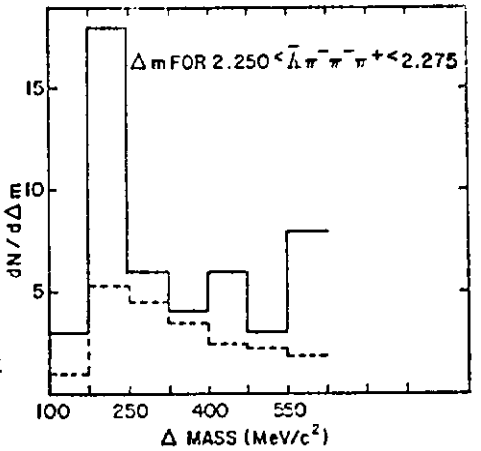

Fig. 7b.

MeV widths typical for conventional states of this mass. There is no peak in $\bar{\Lambda}\pi^+\pi^-\pi^+$ (Fig. 6b). The $\bar{\Lambda}(3\pi)^-$ state has Q = -1, S = 1, B = -1. If strangeness were conserved in the decay to this state (as one would expect for conventional hadrons), the decaying state would have $I_3 = -1$. An $I_3 = +1$, positive charge partner would be expected. The hint of a broad bump in the $\bar{\Lambda}(3\pi)^+$ spectrum has been studied carefully by Monte Carlo and is caused by reflections from $\bar{\Lambda}(3\pi)^- + n\pi^\pm$. A narrow peak at 2.25 ± .05 GeV in $\bar{\Lambda}(3\pi)^-$ with none in $\bar{\Lambda}(3\pi)^+$ is predicted for the $\bar{\Lambda}_c^-$ (cud quarks I = 0) by the charm model (DeRujula, Georgi, Glashow, and Sakharov).[4] The peak is dramatic confirmation of this prediction and represents the first observation of a charmed (anti-) baryon.

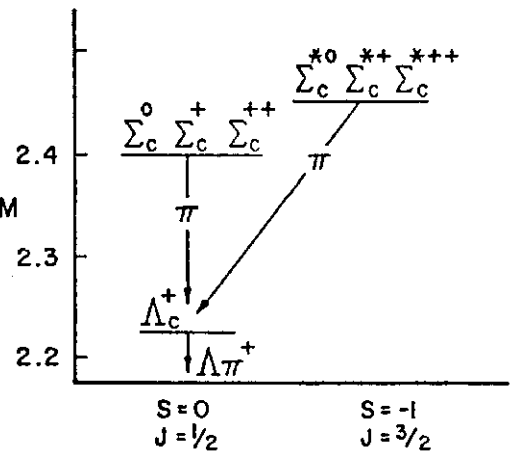

Fig. 8.

There is little observable structure in $\bar{\Lambda}(4\pi)^0$ (Fig. 7a) except for the suggestion of a peak at 2.45 GeV in $\bar{\Lambda}(4\pi)^0$. If one selects all $\bar{\Lambda}(3\pi)^-$ in the 2.26 GeV peak one finds a strong correlation with 2.45 GeV in $\bar{\Lambda}(4\pi)^0$, as seen in Fig. 7b. Δm is the mass difference between $\bar{\Lambda}(4\pi)^0$ and $\bar{\Lambda}(3\pi)^-$. The dashed line shows events just outside the 2.26 GeV peak. This is interpreted as evidence for a cascade from $\bar{\Sigma}_c$ (or $\bar{\Sigma}_c^*$) to $\bar{\Lambda}_c$ + π (Fig. 8). Taking detection efficiency into account this cascade apparently leads to > 50% of $\bar{\Lambda}_c$. One recalls a neutrino event seen by Samios and colleagues in the Brookhaven

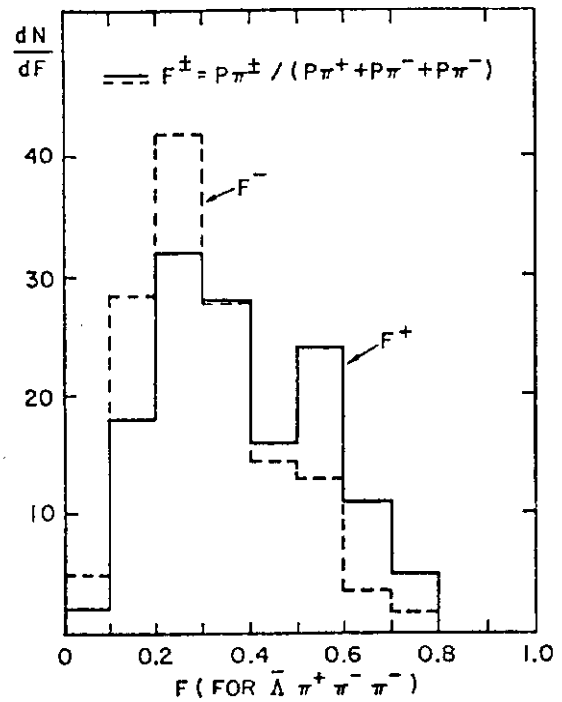

Fig. 9.

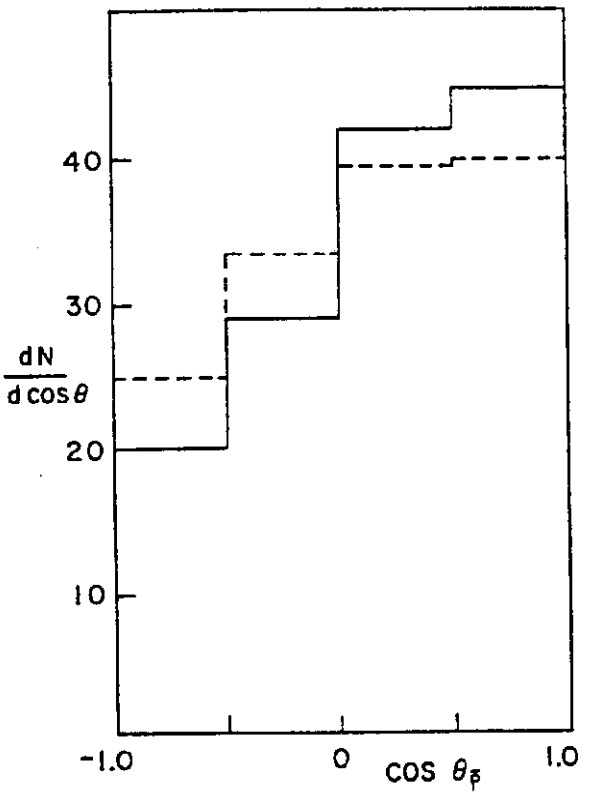

Fig. 10.

bubble chamber: $\Lambda^{o}(4\pi)^{++}$ (2.426 GeV) → $\Lambda^{o}(3\pi)^{+}$ (2.244 GeV) + π^{+}. The similarity is impressive.

The cross section for $\bar{\Lambda}_c$ production and decay to the $\bar{\Lambda}(3\pi)^{-}$ state has been estimated with some difficulty. The greatest uncertainty is in the triggering efficiency which may be anywhere from 10% to 100%. For this range σ x BR = 34 to 340 nb/Be nucleus.

What else has been learned about the $\bar{\Lambda}_c$? It does not appear to be produced often with leptons though 15-20% of such occurrences cannot be ruled out. The π^{+} tends to be produced more energetically than the π^{-} in the decay (Fig. 9), consistent with the "soft pion theorem". There is evidence at the 2 σ level for parity violation in the decay by comparing the forward-backward $\bar{p}$ asymmetry in the peak (solid line) with that near the peak (dashed line)(Fig. 10). This would point to a weak decay as expected for the lowest mass charmed antibaryon. The $\bar{\Lambda}_c$ is apparently produced with other charged particles. There are five times as many events with at least one positive

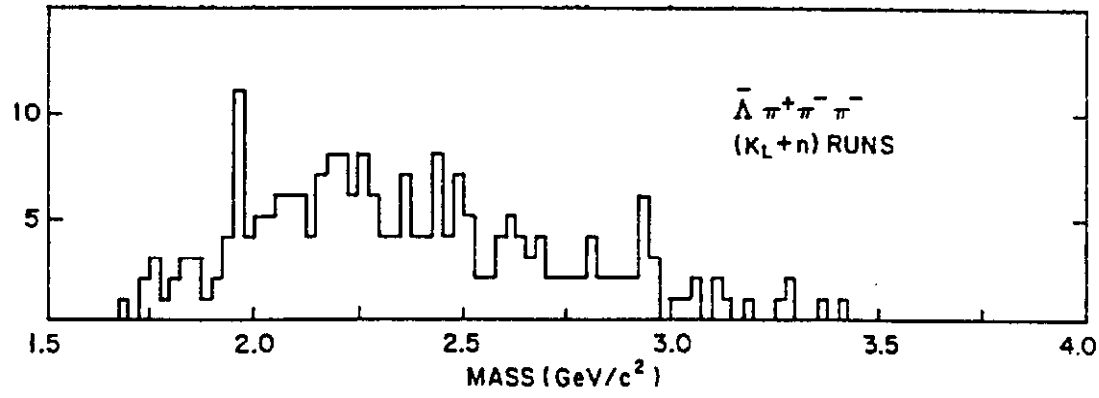

Fig. 11.

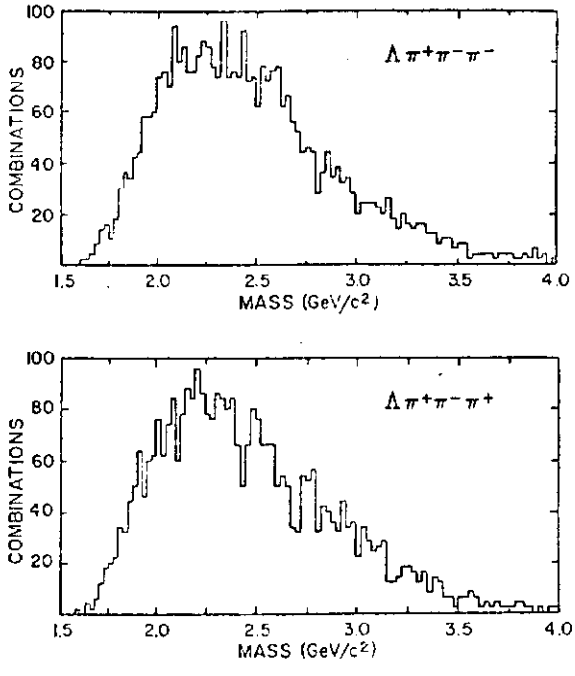

Fig. 12.

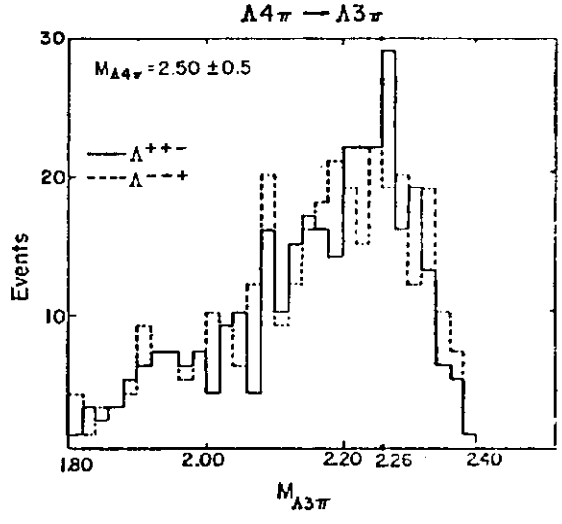

Fig. 13

spectator as events with at least one negative spectator. The positive tracks have high momentum and may well be protons.

The $\bar{\Lambda}_c$ is indeed produced by photons. If the photons in the beam are stopped upstream, the remaining K_L,n beam produces no peak (Fig. 11).

Regrettably, there is no peak corresponding to the $\bar{\Lambda}_c$ in the baryon spectrum, $\Lambda(3\pi)^+$ (nor in $\Lambda(3\pi)^-$). See Fig. 12. Can one learn how to enhance the $\bar{\Lambda}_c$ in the data and then apply the techniques to the baryon spectrum? The best that can be done along these lines is to select events around 2.45 GeV in the $\bar{\Lambda}(4\pi)$ spectrum and look at $\bar{\Lambda}(3\pi)$. This strongly enhances the

$\bar{\Lambda}_c$ peak. Doing the same for the baryons leaves a marginal 10 events over background at 2.26 GeV where one would have expected 20 (Fig. 13).

The lack of a strong Λ_c peak is due to a combination of several possible causes. The most important is the fact that the continuum in the baryon spectrum is about three times higher than in the antibaryon spectrum. This undoubtably results from the excess of baryons in the target and beam. This larger background combined with a statistical fluctuation conspiracy enhancing the $\bar{\Lambda}_c$ and reducing the Λ_c is one possible explanation for the apparent comparative weakness of any Λ_c signal. It is also possible that the difference in production or decay of the Λ_c and $\bar{\Lambda}_c$ might have lead to the Λ going more forward than the $\bar{\Lambda}$ and thereby resulting in a lower spectrometer acceptance for the Λ_c events. This could result from a CP violating process, for example, or simply different production energy distributions for Λ_c and $\bar{\Lambda}_c$.

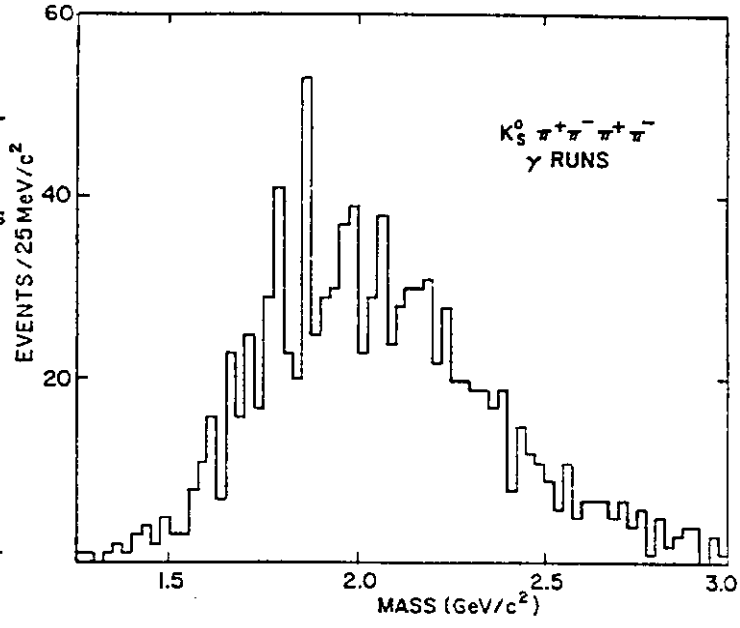

Fig. 14.

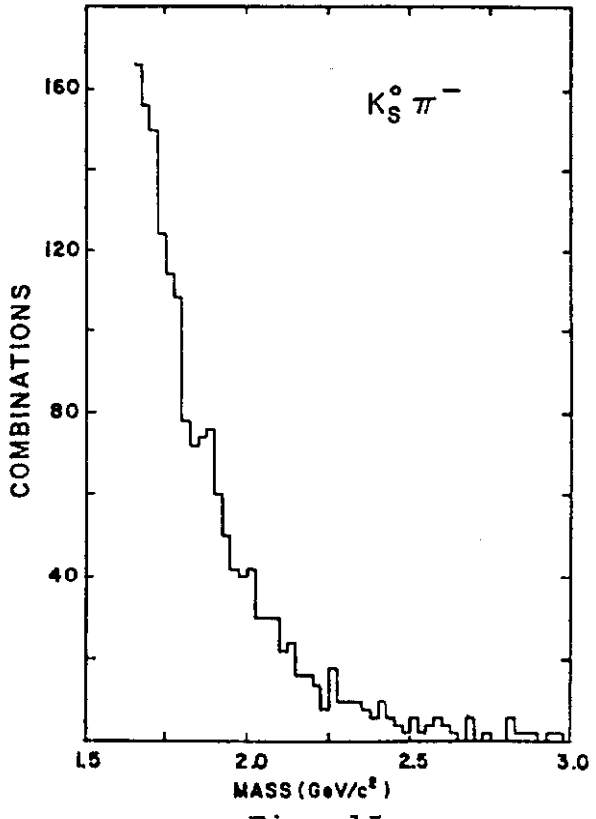

Fig. 15.

I promised that I would show spectra for all states with high mass structure. Figure 14

shows the K_s^o $(4\pi)^o$ distribution. This has been enhanced by limiting the energy of the state to below 150 GeV and using only 6 prong events. The result is a 4 or 5 σ single channel peak at 1.86 GeV (width ~ 25 MeV) which corresponds to the D^o charmed meson observed first at SPEAR. There is also, at least to me, a suggestive shoulder near this mass in the K_s^o π^- spectrum (Fig. 15).

Let me discuss now the very recently analyzed results from the Toronto-Santa Barbara-Fermilab group on the hadronic photoproduction total cross section on hydrogen. This group consists of J. Cumalat (thesis), D. Caldwell, P. Davis, R. Egloff, A. Eisner, A. Lu, G. Luste, J. Martin, R. Morrison, F. Murphy, T. Nash, J. Prentice and S. Yellin. The analysis work is still going on and the results are so recent that they must be considered preliminary.

This is a very fundamental experiment which was designed primarily to see if the photon cross section behaves like that of other hadrons. At the Bonn Conference in 1973 $\sigma_{\gamma p}$ was projected to follow the ρp cross section estimated from the quark model to go as $1/2\ (\sigma_{\pi^+ p} + \sigma_{\pi^- p})$.[5] Of more recent interest is the question of the extent to which charm will show up in the total cross section. There are several ways of estimating this which tend to lead to a similar - perhaps surprising - conclusion. Taking into account quark charges, one finds that the photon couples to a charm-anti charm pair ~ 40% of the time (Fig. 1). The experiments measuring J/ψ photoproduction have found $\sigma_{\psi p} \tilde{\sim} 1.2$ mb using vector dominance arguments. This is ~ 1/20 of $\sigma_{\pi p}$, so one can estimate the total charm photoproduction cross section to be the order of 1/20 x 40% $\simeq$ 2% of the total cross section (~ 2 μbarns).

A precise experiment - statistical and systematic errors < 1% - is required to have a chance to see effects like these. The advantages of high energy photon physics mentioned earlier have made it possible to reach such levels of precision in this experiment and have error bars some 3 times smaller than in the lower energy experiments.

All three terms that contribute to the cross section:

$$\sigma = (\text{target constants}) \times \frac{\text{hadronic events}}{\text{number of photons}}$$

must be known with precision. The target was 1.00027 meters of liquid hydrogen separated from the beam and experiment vacuum by a total of 200 μ of mylar windows at each end. The temperature was measured by 4 platinum resistors to be typically $20.4^{\circ} \pm .2$. Two pressure transducers measured the

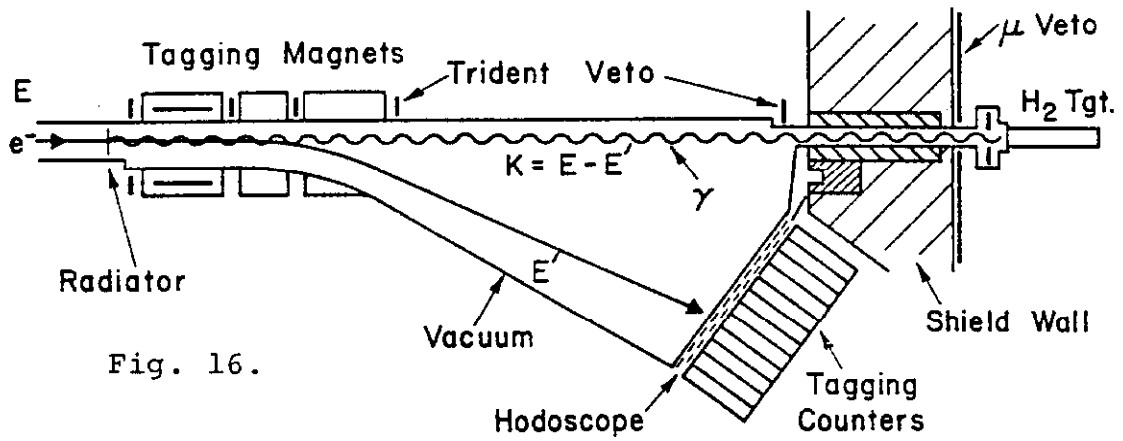

Fig. 16.

vapor pressure and thereby the temperature, independently, to be $20.5^{\circ} \pm .2$. By analysis the D_2 (etc.) contamination was $\lesssim .01\%$. The density was thus known to $\pm \lesssim .2\%$ and the length to better than $\pm .05\%$.

The photon tagging system (Fig. 16) counted the number of photons on target as a function of energy. False tags (tagging signal with no photon) were kept below .05% (!). This was accomplished by vetoing positrons which were bent to the side away from the electrons into a set of veto counters. This eliminated trident like events in which the photon internally or externally converted to e^+e^-. Double bremsstrahlung requires a correction because there are more photons available than tagged. This correction is roughly equal in magnitude to the thickness of the radiator in radiation lengths. To keep the correction small, thin radiators (~ ½% X_o, ~ 1% X_o and ~ 2½% X_o) were used. Runs were taken at different thicknesses to allow a check on the double bremsstrahlung correction. An example of the very clean signal from a typical tagging lead

glass channel is shown in Fig. 17. There is no evidence of π contamination.

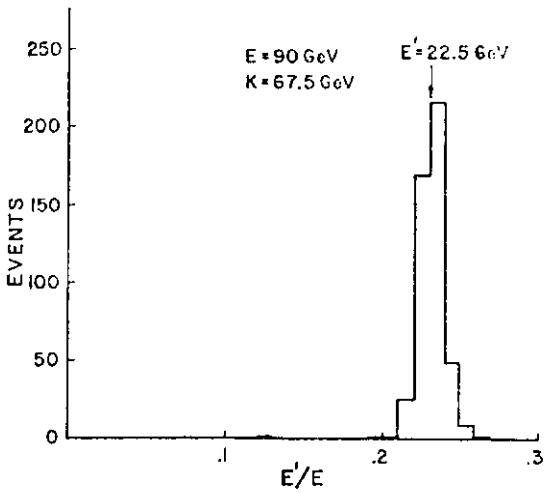

Fig. 17.

The number of hadron interactions is the third major factor of the equation for the total cross section. Note that this is <u>not</u> a transmission measurement as is usual in σ_T experiments in p, π, or K beams. On hydrogen the QED cross section for e^+e^- pairs is ~ 20 mbarns, almost 200 times the hadronic cross section. A transmission measurement would give only the radiation length. Counting hadronic interactions in the face of the overwhelming electromagnetic background is the fundamental challenge of the experiment. For a .2% measurement a rejection of 10^5 is needed.

In pair production essentially all the photon energy is carried away at almost exactly 0^o by the electrons. Energy is partitioned between the pair in a nearly flat distribution. Thus at 100 GeV only ~ 2% of the time does one of the pair have < 2 GeV and thus is multiply scattered out of a 3 mrad cone. The hadronic interaction signature is very different: a) large multiplicities (except known vector mesons, 2 body final states occur < 0.1% of the time); b) large angles (ρ opening angle $\gtrsim 2\,\frac{m}{K} \simeq 16$ mrad @ 100 GeV); c) very little electromagnetic energy (π^o, γ, $e^{\pm}$) at 0^o.

The basic detector arrangement required for this experiment is now clear. A charged and neutral hadron detector should cover the forward center of mass hemisphere with a central hole just safely smaller than the ρ opening angle. Behind this hole an electromagnetic central shower counter should measure 0^o EM energy and veto pair events. The longitudinal detector positions should be scaled for different energy ranges.

The high precision goals of this experiment require more

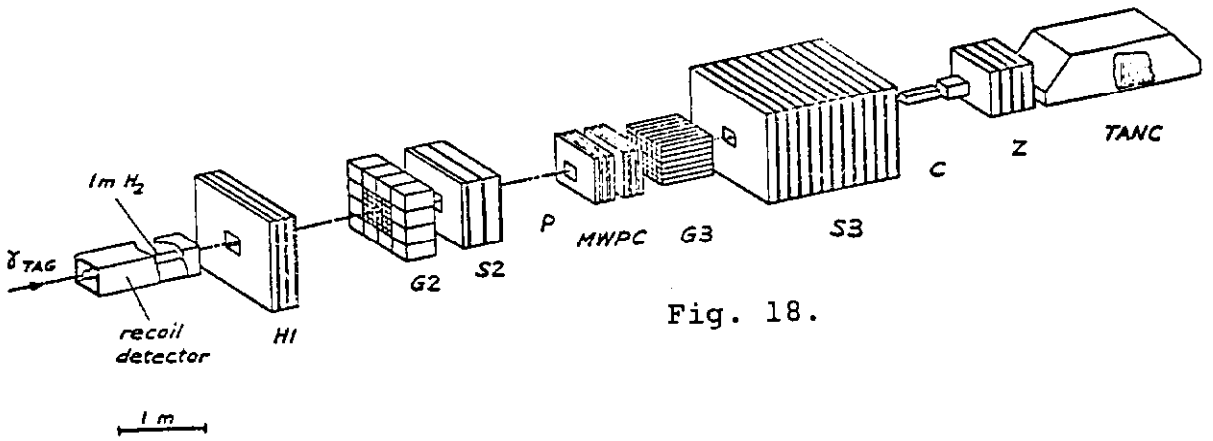

Fig. 18.

Fig. 18. Detector at E_e = 90 GeV

H1 (~ 1½ Absorpt. lengths)
3 planes Fe-scint.

H2 (~ 3 Absorpt. lengths)
G2: 44 blocks 33 cm Pb glass
S2: Pb/scint/Fe/scint/Fe/scint

C lead lucite central shower counter (23 X_o)

H3 (~ 8 Absorpt. lengths)
P: Scint. counter
MWPC: 6 2 mm wire chambers 3 orientations
G3: 7x7 array, 6.4x6.4x58 cm Pb glass. I=inner ring
S3: 12 planes, Fe-scint.

TANC central hadron calorimeter (~ 3½ Absorpt. lengths)

- -

complexity in the actual detector layout which is shown in its E_e = 90 GeV configuration in Fig. 18. There are three hadron detectors (H_1, H_2, H_3) which provide overlapping coverage of the forward CM hemisphere. Each of the hadron detectors has excellent efficiency for $\pi^o \to \gamma\gamma$ (12-21X_o lead glass in H_2 and H_3) and for p, $\pi^\pm$. Neutrons and K_L^o are detected with ~ 90% efficiency in the lead-steel-scintillator detector, S_2 and with nearly 100% efficiency in S_3. Thresholds of these detectors for hadronic events were (typically): S_1, 5 min. ion. tracks or 3 planes of 1 min. ion.; G_2, .85 GeV; S_2, 3.5 min. ion. or 2 of 3 planes of 1 min. ion.; G_3, 1.5 GeV; S_3, 4 GeV.

Most pairs are detected in the central counter, C, which covers ~ ± 3 mrad in the 90 GeV setting. Low energy $e^\pm$ scattering outside of C and other rare electromagnetic channels

($\gamma e^- \rightarrow \gamma e^-$, for example) are identified with the MWPC and G_3. The central hadrometer (TANC) behind C is used to spot events in which a γ (or $e^{\pm}$) interacts in C as well as to detect hadrons coming through the central hole. Since P · TANC · $\bar{C}$ was the only TANC trigger accepted, γ interactions in C were normally vetoed. Offline identification of confusing events of this type was helped by a phototube looking at the first few samples of the C counter shower light. A large signal there indicates that an e or γ interaction in C has probably occurred rather than a small angle π track.

The hadronic event trigger was H_1 or H_2 or H_3 or $\bar{C}$ · (I or P · TANC). Other scaled down triggers were taken: pairs, non-interacting γ, false tags (an excellent check of the fast logic efficiency since no hadronic events should show up in analysis), and HC.

In the analysis of this experiment the data was divided into 60 classes involving various combinations of detectors, etc. Each class was appropriately assigned to either the hadronic or EM category. Despite the large number of classes used for study purposes, the hadronic cross section is dominated by just a few obvious multidetector classes. For example, at E_e = 135 GeV the only hadronic classes with more than 1% of the events were $H_1H_2H_3$ (~60%), $H_1G_2S_2$ (~20%), H_2H_3 (~12%), H_1H_3 (~6%), and H_1S_2 (~2%).

The fraction of the beam photon energy in the C counter (E_C/E_γ) demonstrates the clean separation of hadronic and EM events in the experiment. Figure 19a shows pair events peaking at E_C/E_γ = 1. There are very few pair events below .7. Figure 19b shows this plot for all hadronic triggers (except events with the I or TANC counters on for which E_{IC}/E_γ is more relevant). EM events allowed by the loose hadronic trigger are seen peaking at E_C/E_γ = 1 and are clearly separated from the hadronic events, the great majority of which are near 0. A cut of .7 has been used in most hadronic classes. (In a few low cross section classes E_{IC} or lower cuts on E_C were used). Very few hadronic events are lost by this cut as can be seen

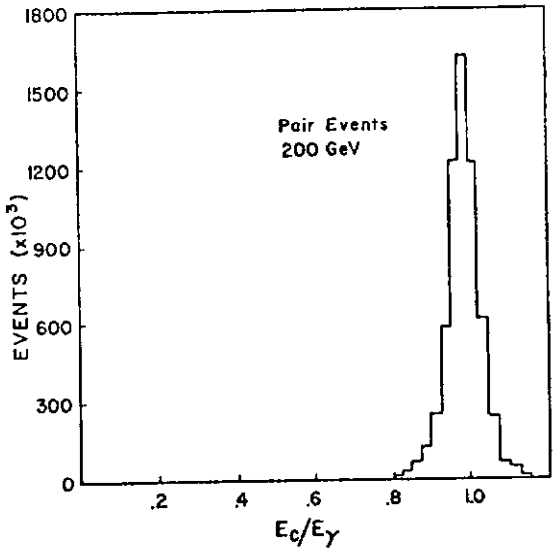

Fig. 19a.

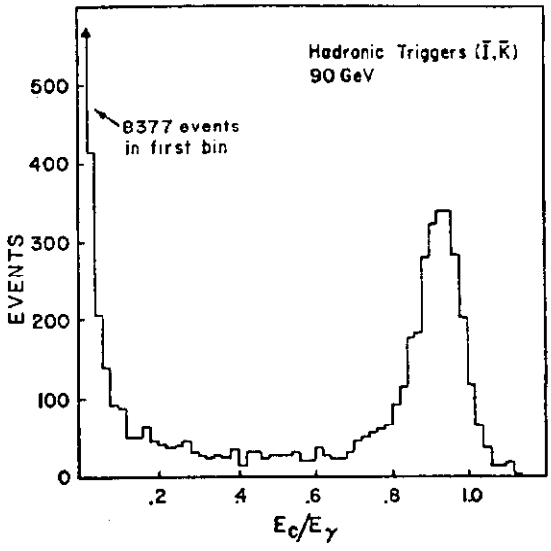

Fig. 19b.

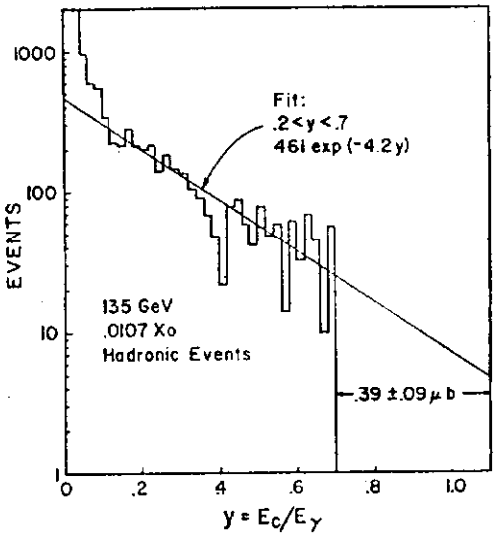

Fig. 20.

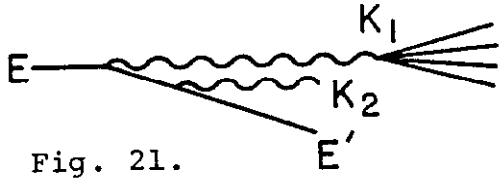

Fig. 21.

in Fig. 20. Here all hadronic events are shown on a log scale (corrected for double bremsstrahlung). A projection into the cut region indicates a loss of 0.39% for this typical sample of data. The slope and magnitude of events in this plot can be predicted from π inclusive and electroproduction data in good agreement with the γ data.

Multiple bremsstrahlung (Fig. 21) requires a correction of ~ 1% (2.5% for the .0268 X_o radiator). If k_1 interacts and $k_1 \geq .5E_\gamma$ the event is included since above 30 GeV the cross section and acceptance are very little different at .5k and at k. If $k_2 > .7\ E_\gamma$ the event is vetoed by the E_c/E_γ cut. Therefore, in this preliminary analysis a correction has been made for events with $.3 < k_1/E_\gamma < .5$.

Data was taken at electron beam energies of 40, 60, 90, 135 and 200 GeV with the detectors positions appropriately

scaled for each energy. At 40 and 60 GeV the G_2 detector was removed for space reasons. At each setting, photon energies overlap more than 50% of the range of the neighboring setting. This provides a critical check of many facets of the experiment such as acceptance and detector stability. An additional check was provided by a second 90 GeV run with the H_1 and H_2 detectors pushed backwards and a second 60 GeV run with detectors at the 90 GeV position (including G_2). As a check on the double bremsstrahlung correction and other radiator dependent effects, data was taken with several tagging radiator thicknesses. At 135 and 200 GeV, where γ flux was limited, radiators of $.0107X_o$ and $.0268X_o$ were used. At 90 GeV thicknesses were $.0107X_o$ and $.0054X_o$. At 60 and 40 GeV, $.0107X_o$ was used.

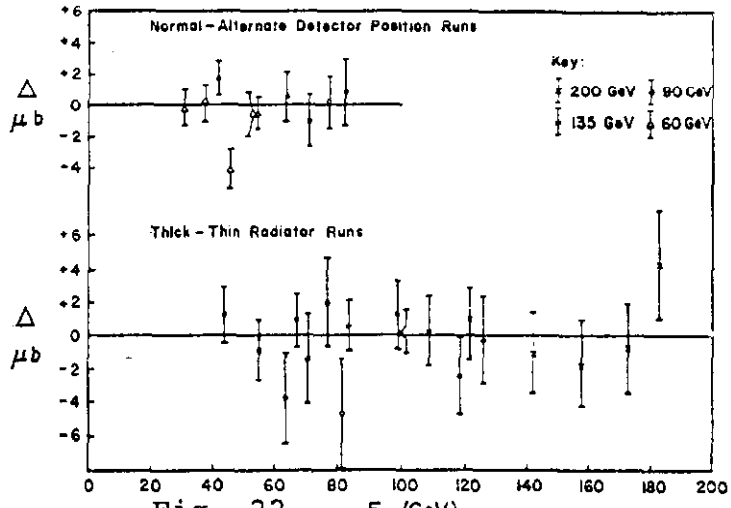

Fig. 22.

The differences in the cross section result (Δ) for the thin and thick radiator runs and the normal and alternate detector positions at the various energies are shown in Fig. 22. There is clearly excellent agreement within statistics between the various runs. The combined data is shown in Fig. 23 with a magnified vertical scale broken at 100 μb. Where they overlap the data from different energy regions agree well. As noted earlier, this is a very important check on the experiment since the detector configuration varies radically between different settings.

A fit to the data for $30 < E_\gamma < 185$ GeV gives $\sigma = (113.21 \pm .37) + (.0267 \pm .0047)\ E_\gamma$ μb with $\chi^2 = 55$, $n_D = 52$. The results from this experiment should be treated as preliminary, as they are very recent and the data is still being studied. Systematic errors are presently estimated to be 0.8%, energy independent, and 0.4%, energy dependent.[10]

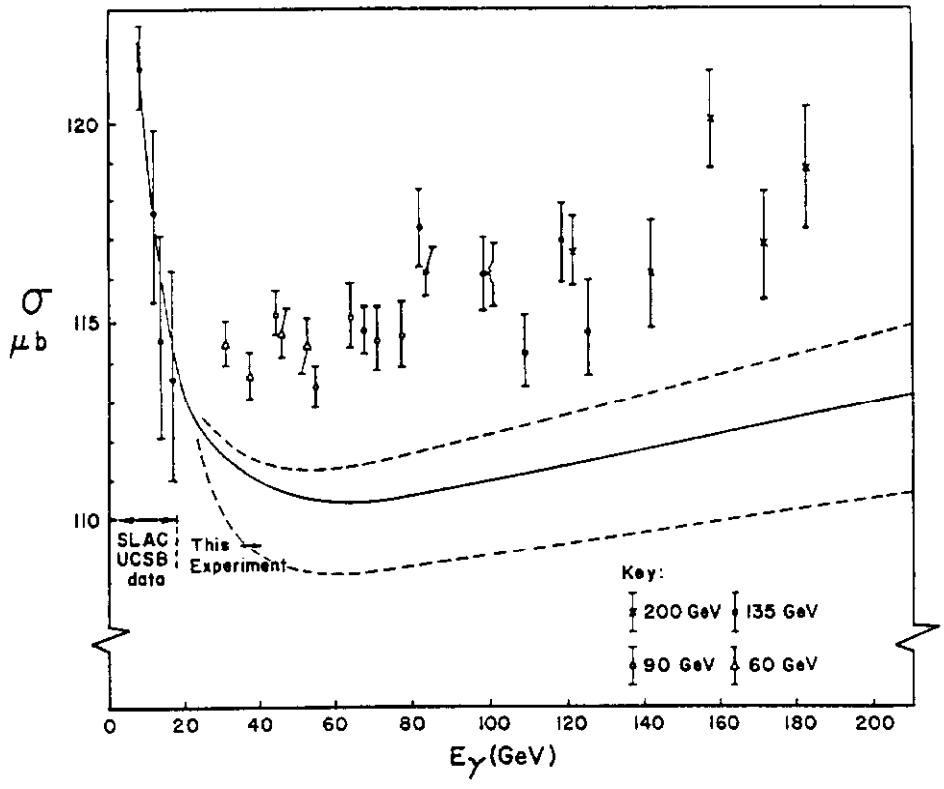

Fig. 23.

The energy dependence of the vector meson - proton cross section can be deduced from the quark model relations:

$$\sigma_{\rho p} = \sigma_{\omega p} = \tfrac{1}{2}[\sigma_{\pi^+ p} + \sigma_{\pi^- p}]$$

$$\sigma_{\phi p} = \sigma_{K^+ p} + \sigma_{K^- p} - \sigma_{\pi^- p}$$

Vector dominance considerations suggest that $\sigma_{\gamma p}$ has the energy dependence of an appropriate linear combination of σ_{Vp}. Traditional projections into this energy range assumed $\sigma_{\gamma p}$ = const $\sigma_{\rho p}$.[5] This projection is shown in the lowest, dashed, curve in Fig. 23. Data on $\sigma_{\pi^\pm p}$[6] from the PS, AGS, Serpukhov and Fermilab were used and $\sigma_{\rho p}$ was normalized to fit the SLAC $\sigma_{\gamma p}$ data below 20 GeV.[11] Obviously missing from this projection is $\sigma_{\phi p}$. The top two curves in Fig. 23 show $\sigma_{\gamma p} = c[(\gamma_\rho^{-2} + \gamma_\omega^{-2})\sigma_{\rho p} + \gamma_\phi^{-2}$ $\sigma_{\phi p}]$ using $K^\pm p$ data from the same experiments.[6] There is some question on what value to use for γ_ϕ^2 since results from the colliding beams at $q^2 = m_\phi$ are not the same as those from A dependent photoproduction ($q^2 = 0$).[7] The solid curve uses the $q^2 = 0$ coupling constants which is most appropriate for comparison with $\sigma_{\gamma p}$ measured at $q^2 = 0$. The upper, dashed, curve

uses colliding beam constants and indicates the upper range of projections that do not invoke charm. Note that there may be as much as a 1½ μb systematic normalization error in any of these projected curves because of uncertainties in the low energy photoproduction data and the normalization differences between the different πp or Kp experiments.

We noted earlier the expectation that the total charm photoproduction cross section is around 1 or 2 μbarn. The difference between the $\sigma_{\gamma p}$ measurement at high energy and the quark model projections without charm is certainly consistent with 1 or 2 μbarn of charm and perhaps more. Measurements of $\sigma(\gamma p \to J/\psi)$ at Fermilab and SLAC indicate that σ_ψ rises by over a factor of three between 20 and 50 GeV.[8] Above 80 GeV the cross section has been observed to continue a slow rise.[9] The high energy $\sigma_{\gamma p}$ data appears to point down toward an intersection with the SLAC data near 20 GeV. This is just the behavior expected if the charm cross section increases rapidly between 20 and 40 GeV as suggested by the J/ψ results, and if there is a small normalization difference between the low and high energy experiments. The slope of the σ_T data is somewhat higher than the slope of the projected curves. Given the slow rise of σ_ψ at high energy, this is also consistent with the idea that charm quarks are causing the apparent excess in σ_T over the projections.

The σ_T data taken at E = 40 GeV are now being analyzed and will be available shortly. They will fill the gap between 30 and 20 GeV. This will contribute to a better understanding of the systematic uncertainties between the SLAC and Fermilab σ_T experiments and, perhaps, reinforce the interpretation of the preliminary results I have just given.

I would like to thank W. Lee and M. Gormley for discussions and the latest data from the Broad Band photon experiment. I would also like to thank my colleagues on the photon total cross section experiment for allowing me to speak about our early results.

References

1. M. K. Gaillard, B. W. Lee, J. L. Rosner, Rev. Mod. Phys. 47, 277 (1975).
2. B. Knapp, et al., Phys. Rev. Letters 37, 882 (1976). P. S. Leung, Ph.D. Thesis, Columbia University (1977), unpublished, Nevis 220.
3. B. Knapp, et al., Phys. Rev. Letters 34, 1040 (1975).
4. A. DeRújula, H. Georgi, S. L. Glashow, Phys. Rev. D12, 147 (1975). A. D. Sakharov, JETP Lett. 21, 258 (1975).
5. E. Gabathulier in Proceedings of the VIth International Symposium on Electron and Photon Interactions at High Energies, Bonn (1973), p 309.
6. A. S. Carroll, et al., Phys. Letters 61B, 303 (1976); S. P. Denisov, et al., Phys. Letters 36B, 415 (1971); S. P. Denisov, et al., Nucl. Phys. B65, 1 (1973); K. J. Foley, et al., Phys. Rev. Letters 19, 330 (1967); H. W. Galbraith, et al., Phys. Rev. 138B, 913 (1965).
7. A. Silverman in Proceedings of the 1975 International Symposium on Lepton and Photon Interactions at High Energy, Stanford (1975), p 360.
8. U. Camarini, et al., Phys. Rev. Letters 35, 483 (1975); T. Nash, et al., Phys. Rev. Letters 36, 1233 (1976).
9. J. S. Sarracino, Ph.D. Thesis, University of Illinois (1976), unpublished.
10. The first analysis of the 60 GeV data was completed just before this meeting and it is possible that the systematic errors are slightly higher for these points.
11. D. O. Caldwell, Phys. Rev. D7, 1362 (1973). Fits to Serpukhov data are reported in A. Belousov et al., Sov. J. Nucl. Phys., 21, 289 (1975).